

# Analysis of Cascaded H-Bridge Multilevel Inverter with Distributed MPPT for Grid-Connected PV Applications

Madithati Mallikarjuna Reddy<sup>1</sup>, V.Pratapa Rao<sup>2</sup>

<sup>1</sup> PG Student, Dept. of EEE, Sri Sai Institute of Technology & Science, Rayachoty.

<sup>2</sup> Assistant Professor and HOD, Dept. of EEE, Sri Sai Institute of Technology & Science, Rayachoty.

## Abstract:

A modular cascaded H-bridge multilevel inverter for single- or three-phase grid-connected PV applications has been presented in this paper. The modular cascaded multilevel topology helps to improve the efficiency and flexibility of PV systems. To realize better utilization of PV modules and maximize the solar energy extraction, a distributed maximum power point tracking control scheme is applied to both single-phase and three-phase multilevel inverters, which allows independent control of each dc-link voltage. For three-phase grid-connected PV applications, PV mismatches may introduce unbalanced supplied power, leading to unbalanced grid current. To solve this problem, a control scheme with modulation compensation is also proposed. The simulated three-phase seven-level cascaded H-bridge inverter has been built utilizing nine H-bridge modules (three modules per phase). Each H-bridge module is connected to a 185 W PV panel. Simulation results are presented to verify the feasibility of the proposed approach.

**Keywords-** Cascaded multilevel inverter, distributed maximum power point tracking, modulation compensation, photovoltaic system.

## 1. Introduction

DUE to the shortage of fossil fuels and environmental problems caused by conventional power generation, renewable energy, particularly solar energy, has become very popular. Solar-electric-energy demand has grown consistently by 20%–25% per annum over the past 20 years, and the growth is mostly in grid-connected applications [1-3]. With the extraordinary market growth in grid-connected photovoltaic (PV) systems, there are increasing interests in grid-connected PV configurations. Five inverter families can be defined, which are related to different configurations of the PV system: 1) central inverters; 2) string inverters; 3) multi-string inverters; 4) ac-module inverters; and 5) cascaded inverters. The configurations of PV systems are shown in Fig.1. Cascaded inverters consist of several converters connected in series; thus, the high power and/or high voltage from the combination of the multiple modules would favor this topology in medium and large grid-connected PV systems. There are two types of cascaded inverters. Fig. 1(e) shows a cascaded dc/dc converter connection of PV modules. Each PV module has its own dc/dc converter, and

the modules with their associated converters are still connected in series to create a high dc voltage, which is provided to a simplified DC/AC inverter [4]. This approach combines aspects of string inverters and ac-module inverters and offers the advantages of individual module maximum power point (MPP) tracking (MPPT), but it is less costly and more efficient than ac-module inverters. However, there are two power conversion stages in this configuration. Another cascaded inverter is shown in Fig. 1(f), where each PV panel is connected to its own dc/ac inverter, and those inverters are then placed in series to reach a high-voltage level.

This cascaded inverter would maintain the benefits of “one converter per panel,” such as better utilization per PV module, capability of mixing different sources, and redundancy of the system. In addition, this DC/AC cascaded inverter removes the need for the per-string DC bus and the central DC/AC inverter, which further improves the overall efficiency [5,6]. The modular cascaded H-bridge multilevel inverter, which requires an isolated dc source for each H-bridge, is one dc/ac cascaded inverter topology. The separate DC links in the multilevel inverter make independent voltage

control possible [7]. As a result, individual MPPT control in each PV module can be achieved, and the energy harvested from PV panels can be maximized. Meanwhile, the modularity and low cost of multilevel converters would position them as a prime candidate for the next generation of efficient, robust, and reliable grid connected solar power electronics.

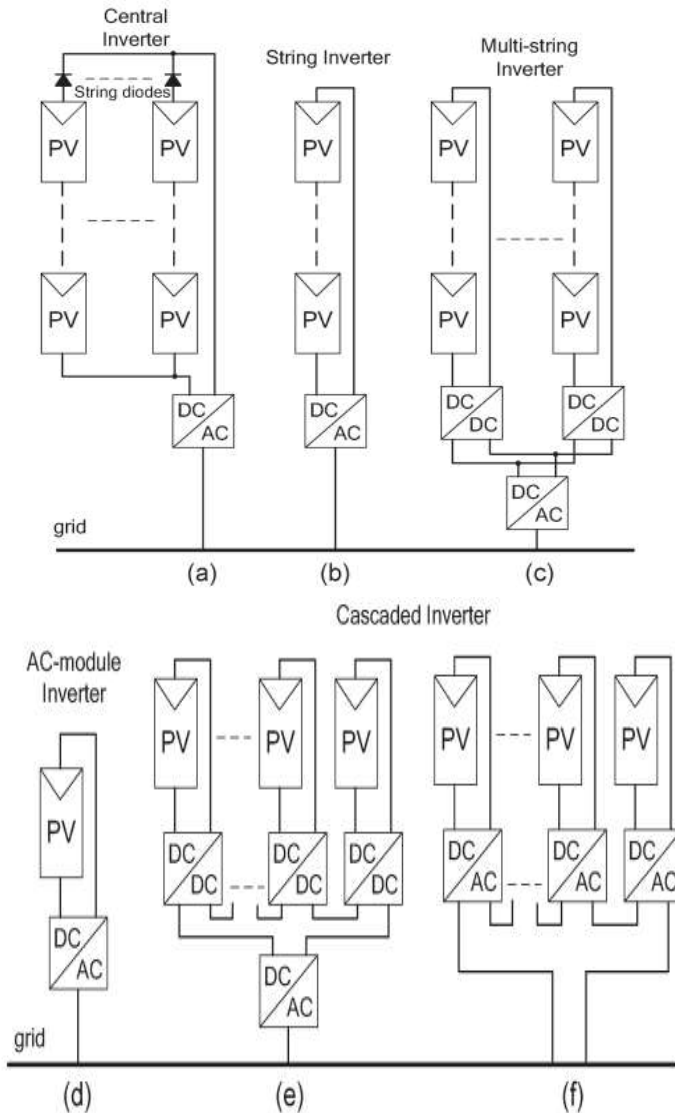


**Figure 1: PV system Inverter configurations. (a) Central inverter. (b) String inverter. (c) Multi string inverter. (d) AC-module inverter. (e) Cascaded DC/DC converter. (f) Cascaded DC/AC inverter.**

A modular cascaded H-bridge multilevel inverter topology for single- or three-phase grid-connected PV systems is presented in this paper. The panel mismatch issues are addressed to show the necessity of individual MPPT control, and a control scheme with distributed MPPT control is then proposed. The distributed MPPT control scheme can be applied to both single and three-phase systems. In addition, for the presented three-phase grid-connected PV system, if each PV module

is operated at its own MPP, PV mismatches may introduce unbalanced power supplied to the three-phase multilevel inverter, leading to unbalanced injected grid current.

To balance the three-phase grid current, modulation compensation is also added to the control system. A three-phase modular cascaded multilevel inverter prototype has been built. Each H-bridge is connected to a 185 W solar panel. The modular design will increase the flexibility of the system and reduce the cost as well. Simulation results are provided to demonstrate the developed control scheme.

### 1.1. Literature survey

#### Power-electronic systems for the grid integration of renewable energy sources: A survey

The use of distributed energy resources is increasingly being pursued as a supplement and an alternative to large conventional central power stations. The specification of a power-electronic interface is subject to requirements related not only to the renewable energy source itself but also to its effects on the power-system operation, especially where the intermittent energy source constitutes a significant part of the total system capacity. In this paper, new trends in power electronics for the integration of wind and photovoltaic (PV) power generators are presented. A review of the appropriate storage-system technology used for the integration of intermittent renewable energy sources is also introduced. Discussions about common and future trends in renewable energy systems based on reliability and maturity of each technology are presented.

#### A review of single-phase grid connected inverters for photovoltaic modules

This review focuses on inverter technologies for connecting photovoltaic (PV) modules to a single-phase grid. The inverters are categorized into four classifications: 1) the number of power processing stages in cascade; 2) the type of power decoupling between the PV module(s) and the single-phase grid; 3) whether they utilize a transformer (either line or high frequency) or not; and 4) the type of grid-connected power stage. Various inverter topologies are presented, compared, and evaluated against demands, lifetime, component ratings, and cost. Finally, some of the topologies are pointed out as the best candidates for either single PV module or multiple PV module applications.

#### String and module integrated inverters for single-phase grid connected photovoltaic systems

This work presents an overview on recent developments and a summary of the state-of-the-art in inverter technology for single-phase grid connected photovoltaic (PV) systems. The information provided includes details on commercially available European string and module integrated PV inverters, their efficiency, price trends and market share. This review is given for inverters for a power level up to 6 kW. Furthermore, the project deals with the recent developments of new inverter topologies and PV system concepts and discusses possible future trends.

### Photovoltaic DC-building-module-based BIPV system—Concept and design considerations

The photovoltaic (PV) modules used in the building-integrated PV (BIPV) system, generally, can be installed in different orientations and angles. Moreover, performance of the PV modules is easy to be affected by partial shadows and mismatch of their electrical parameters. Consequently, the conventional power configurations are difficult to obtain higher energy efficiency and reliability. Some improved power configurations of BIPV system have been presented to solve these problems. The objective of the project is to give an overview of the existing solutions, and then, proposes an efficient and cost-effective power configuration of BIPV system from the energy conversion and control point of view. The proposed power configuration consists of plenty of PV dc-building module (PV-DCBM) and a centralized inverter. Each PV-DCBM includes a high step-up dc-dc converter integrated with a PV module into an individual electrical device. The PV-DCBMs are parallel connected, and then, connected to a common dc bus. The centralized inverter is connected to the grid. The design criterions, optimum design considerations, and design procedure of the proposed PV-DCBM-based BIPV system are proposed in this paper. The experimental results are presented to verify the validity and feasibility of the novel concept.

**Multilevel converters as a utility interface for renewable energy systems** Multilevel inverter structures have been developed to overcome shortcomings in solid-state switching device ratings so that they can be applied to high-voltage electrical systems. The general function of the multilevel inverter is to synthesize a desired AC voltage from several levels of DC voltages. For this reason, multilevel inverters are ideal for connecting either in series or in parallel an AC grid with renewable energy sources such as photovoltaic's or fuel cells or with energy storage devices such as capacitors or

batteries. In this project the cascaded H-bridges multilevel inverter is described.

### 1.2 Problem identification

Cascaded inverters consist of several converters connected in series; thus, the high power and/or high voltage from the combination of the multiple modules would favor this topology in medium and large grid-connected PV systems. There are two types of cascaded inverters. Fig. 1(e) shows a cascaded dc/dc converter connection of PV modules. Each PV module has its own dc/dc converter, and the modules with their associated converters are still connected in series to create a high dc voltage, which is provided to a simplified dc/ac inverter. This approach combines aspects of string inverters and ac-module inverters and offers the advantages of individual module maximum power point (MPP) tracking (MPPT), but it is less costly and more efficient than ac-module inverters. However, there are two power conversion stages in this configuration. Another cascaded inverter is shown in Fig. 1(f), where each PV panel is connected to its own dc/ac inverter, and those inverters are then placed in series to reach a high-voltage level [13]–[16]. This cascaded inverter would maintain the benefits of “one converter per panel,” such as better utilization per PV module, capability of mixing different sources, and redundancy of the system. In addition, this dc/ac cascaded inverter removes the need for the per-string dc bus and the central dc/ac inverter, which further improves the overall efficiency.

## 2. Design of Photovoltaic System

### 2.1 Photovoltaic Cell and Array Modeling

A PV cell is a simple p-n junction diode that converts the irradiation into electricity. Fig. 2 illustrates a simple equivalent circuit diagram of a PV cell [8]. This model consists of a current source which represents the generated current from PV cell, a diode in parallel with the current source, a shunt resistance, and a series resistance.

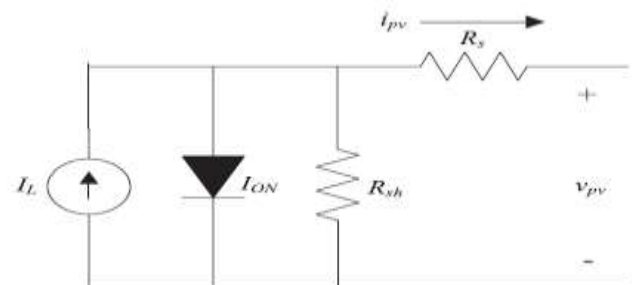


**Figure 2: Equivalent circuit diagram of the PV cell**

From Fig. 2, the diode current can be expressed as

$$I_{ON} = I_s \left[ \exp \left( \frac{q}{AKT_c} (v_{pv} + R_s i_{pv}) - 1 \right) \right] \quad (1)$$

Where  $v_{pv}$  and  $i_{pv}$  are the voltage and current of the PV cell output respectively. Other constants and their definitions are shown in Table 1. The output current, generated by the PV cell, can be calculated by applying Kirchhoff's current law, i.e.

$$i_{pv} = I_L - I_s [\exp[\alpha(v_{pv} + R_s i_{pv})] - 1] - \frac{v_{pv} + R_s i_{pv}}{R_{sh}} \quad (2)$$

In eqn(2.2), the current source output  $I_L$ , is related to the solar irradiation and temperature by

$$I_L = [I_{sc} + k_i(T_c - T_{ref})] \frac{S}{1000} \quad (3)$$

where  $S$  is the solar irradiation,  $I_{sc}$  is the short circuit current,  $k_i$  is the short circuit current coefficient,  $T_c$  is the cell's operating temperature (in K), and  $T_{ref}$  is the reference temperature of the cell.

$$I_s = I_{RS} \left[ \frac{T_c}{T_{ref}} \right]^3 \exp \left[ \frac{qE_g}{Ak} \left( \frac{1}{T_{ref}} - \frac{1}{T_c} \right) \right] \quad (4)$$

where  $I_{RS}$  is reverse saturation current in the reference temperature and solar irradiation, and  $E_g$  is the band gap energy of the PV semiconductor.

**TABLE 1: Parameter values of the considered PV model**

$T_c$	Operation Temperature	298C
$I_{sc}$	Short Circuit Current	3.2A
A	Ideality Factor	1-5
k	Boltzmann's Constant	$1.3807 \cdot 10^{-23}$
q	Electron charge	$1.6022 \cdot 10^{-19}C$
R	Resistance	0.01ohm

Since the output voltage and current of one PV cell are very low, a combination of series and parallel cells are connected together in order to deliver higher current and voltage. These cells are encapsulated with a transparent material to protect them from harsh environmental conditions and form a PV module. In order to obtain a higher voltage and current for higher power applications, a number of PV modules need to be connected to form a PV array as shown in Fig. 3

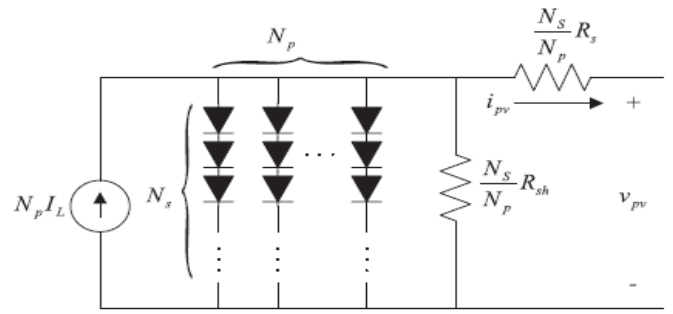


**Figure 3: Equivalent circuit diagram of the PV array**

If number of PV cells connected in series is  $N_s$  and number of PV cells connected in parallel is  $N_p$ ,

then the array output current,  $i_{pv}$  can be expressed as

$$i_{pv} = N_p I_L - N_p I_s \left[ \exp \left[ \alpha \left( \frac{V_{pv}}{N_s} + \frac{R_s i_{pv}}{N_p} \right) \right] - 1 \right] - \frac{N_p}{R_{sh}} \left( \frac{v_{pv}}{N_s} + \frac{R_s i_{pv}}{N_p} \right) \quad (5)$$

## 2.2 Variations in solar irradiation

Usually under the standard atmospheric conditions, the solar irradiation is 1000 W/sq.m. The I-V characteristic of the PV module for different irradiances but under the constant temperature of 25°C are shown in Fig. 4.

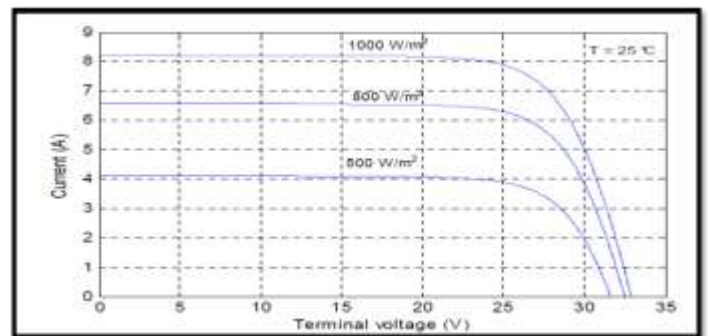


**Figure 4: I-V characteristics of the PV module under different solar irradiation levels**

From Fig. 4, it is observed that, as the solar irradiation increases, the output current increases and the output voltage slightly increases [9,10]. The P-V Characteristics of the PV module for different irradiances under the constant temperature of 25°C are shown in Fig. 5.



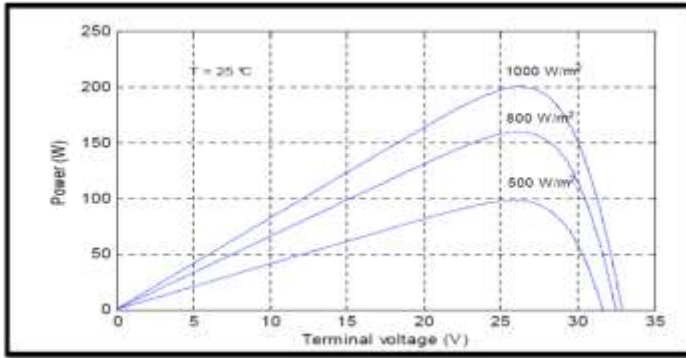


**Figure 5: P-V characteristics of the PV module under different solar irradiation levels**

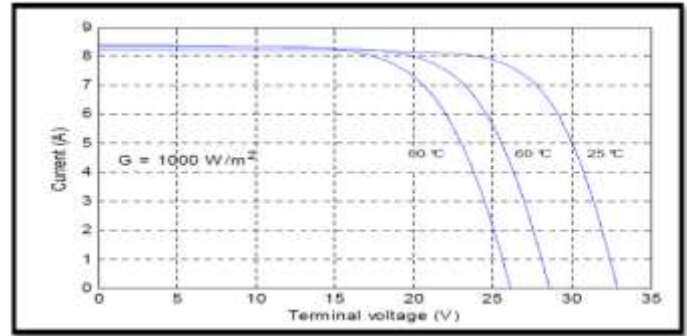


**Figure 6: I-V characteristics of the PV module at different surface temperatures**

### 2.3 Variation in solar cell temperature

Like all other semiconductor devices, solar cells are sensitive to temperature. Increasing the temperature reduces the band gap of a semiconductor, thereby effecting most of the semiconductor material parameters. The decrease in the band gap of a semiconductor with increasing temperature can be viewed as increasing the energy of the electrons in the material. Lower energy is therefore needed to break the bond. In the bond model of a semiconductor band gap, reduction in the bond energy also reduces the band gap. Therefore increasing the temperature reduces the band gap.

A PV module will be typically rated at 25 °C under 1 kW/m<sup>2</sup>. However, when operating in the field, they typically operate at higher temperatures and at somewhat lower isolation conditions. In order to determine the power output of the solar cell, it is important to determine the expected operating temperature of the PV module. The nominal operating cell temperature is defined as the temperature reached by open circuited cells in a module under the conditions as listed below:

1. Irradiance on cell surface = 800 W/m<sup>2</sup>
2. Air temperature = 20°C
3. Wind velocity = 1 m/s
4. Mounting = open back side

In a solar cell, the parameter most affected by an increase in temperature is the open-circuit voltage. Usually under the standard atmospheric conditions, the solar cell temperature is 25°C. The I-V characteristics of the PV module for different temperatures but under the constant solar irradiation of 1000 W/sq.m are shown in Fig. 6. It can also be observed that the variations of the irradiance slightly changes with open-circuit voltage.

From Fig. 7, it is observed that, as the PV module temperature increases, the output current is slightly increases and the output voltage increases. The P-Characteristics of the PV module for different temperatures and with the constant solar irradiation of 1000 W/sq.m are shown in Fig. 7.

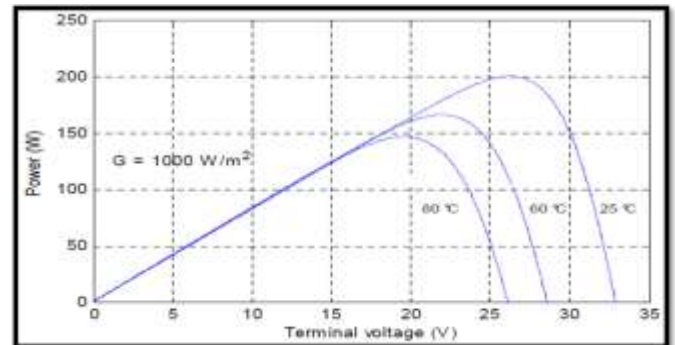


**Figure 7: P-V characteristics of the PV module at different surface temperatures**

## 3. Modeling of Cascaded H-Bridges Inverter

An inverter is an electrical device that converts direct current (DC) to alternating current (AC); the converted AC can be at any required voltage and frequency with the use of appropriate transformers, switching, and control circuits. Static inverters have no moving parts and are used in a wide range of applications, from small switching power supplies in computers, to large electric utility high-voltage direct current applications that transport bulk power [11]. Inverters are commonly used to supply AC power from DC sources such as solar panels or batteries. The electrical inverter is a high-power electronic oscillator. It is so named because early mechanical AC to DC converters was made to work in reverse, and thus was "inverted", to convert DC to AC.

### 3.1 Cascaded H-Bridges inverter

A single-phase structure of an m-level cascaded inverter is illustrated in Fig. 8. Each separate dc source (SDCS) is connected to a single-

phase full-bridge, or H-bridge, inverter. Each inverter level can generate three different voltage outputs,  $+V_{dc}$ , 0, and  $-V_{dc}$  by connecting the dc source to the ac output by different combinations of the four switches,  $S_1$ ,  $S_2$ ,  $S_3$ , and  $S_4$ . To obtain  $+V_{dc}$ , switches  $S_1$  and  $S_4$  are turned on, whereas  $-V_{dc}$  can be obtained by turning on switches  $S_2$  and  $S_3$ . By turning on  $S_1$  and  $S_2$  or  $S_3$  and  $S_4$ , the output voltage is 0 [12]. The ac outputs of each of the different full-bridge inverter levels are connected in series such that the synthesized voltage waveform is the sum of the inverter outputs. The number of output phase voltage levels  $m$  in a cascade inverter is defined by  $m = 2s+1$ , where  $s$  is the number of separate dc sources. An example phase voltage waveform for an 11-level cascaded H-bridge inverter with 5 SDCSs and 5 full bridges is shown in Fig. 9. The phase voltage

$$v_{an} = v_{a1} + v_{a2} + v_{a3} + v_{a4} + v_{a5} \quad (6)$$

For a stepped waveform such as the one depicted in Fig. 9 with  $s$  steps, the Fourier Transform for this waveform follows

$$V(\omega) = \frac{4V_{dc}}{\pi} \sum_n [\cos(n\theta_1) + \cos(n\theta_2) + \dots + \cos(n\theta_s)] \frac{\sin(n\omega t)}{n}, \quad \text{when } n=1,3,5,7,\dots \quad (7)$$

A modular cascaded H-bridge multilevel inverter topology for single or three-phase grid connected PV systems is presented in this paper. The panel mismatch issues are addressed to show the necessity of individual MPPT control with fuzzy logic, and a control scheme with distributed MPPT control is then proposed. The distributed MPPT and fuzzy control scheme can be applied to both single and three-phase systems. In addition, for the presented three-phase grid connected PV system, if each PV module is operated at its own MPP, PV mismatches may introduce unbalanced power supplied to the three-phase multilevel inverter, leading to unbalanced injected grid current [13]. To balance the three-phase grid current, modulation compensation is also added to the control system. A three-phase modular cascaded multilevel inverter prototype has been built. Each H-bridge is connected to a 185W solar panel. The modular design will increase the flexibility of the system and reduce the cost as well. Simulation is provided to demonstrate the developed control scheme.

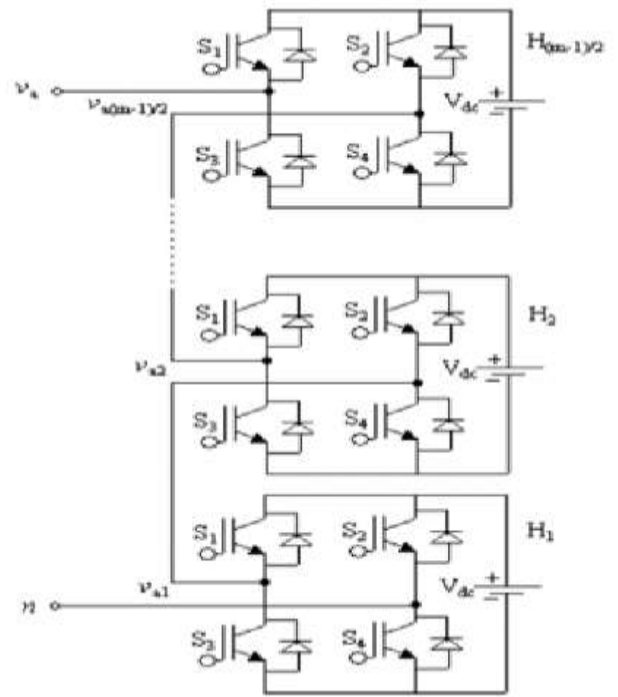


Figure 8: Single-phase structure of a multilevel cascaded H-bridges inverter

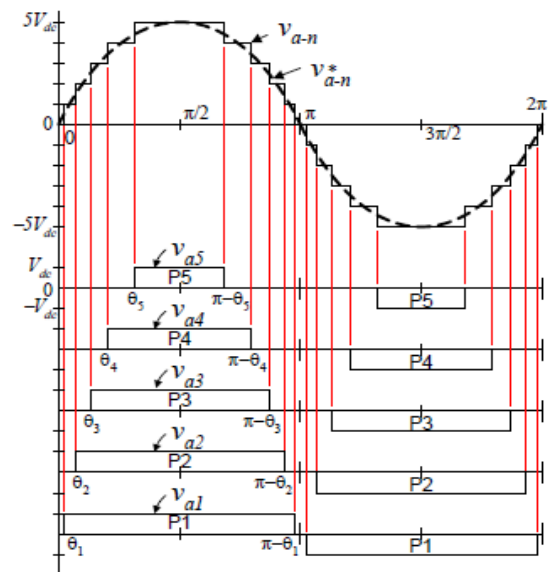


Figure 9: Output phase voltage waveform of an 11-level cascade inverter with 5 separate dc sources.

The magnitudes of the Fourier coefficients when normalized with respect to  $V_{dc}$  are as follows:

$$H(n) = \frac{4}{n\pi} [\cos(n\theta_1) + \cos(n\theta_2) + \dots + \cos(n\theta_s)], \quad \text{when } n=1,3,5,7,\dots \quad (8)$$

The conducting angles,  $\theta_1, \theta_2, \dots, \theta_s$ , can be chosen such that the voltage total harmonic distortion is a minimum. Generally, these angles are chosen so that predominant lower frequency harmonics, 5th, 7th, 11th, and 13, harmonics are

eliminated. More detail on harmonic elimination techniques will be presented in the next section. Multilevel cascaded inverters have been proposed for such applications as static var generation, an interface with renewable energy sources, and for battery-based applications. Three-phase cascaded inverters can be connected in wye, as shown in Fig. 10, or in delta. Peng has demonstrated a prototype multilevel cascaded static var generator connected in parallel with the electrical system that could supply or draw reactive current from an electrical system. The inverter could be controlled to either regulate the power factor of the current drawn from the source or the bus voltage of the electrical system where the inverter was connected.

Peng and Joos have also shown that a cascade inverter can be directly connected in series with the electrical system for static var compensation. Cascaded inverters are ideal for connecting renewable energy sources with an ac grid, because of the need for separate dc sources, which is the case in applications such as photovoltaic's or fuel cells. Cascaded inverters have also been proposed for use as the main traction drive in electric vehicles, where several batteries or ultra capacitors are well suited to serve as SDCSs. The cascaded inverter could also serve as a rectifier/charger for the batteries of an electric vehicle while the vehicle was connected to an ac supply as shown in Fig. 10. Additionally, the cascade inverter can act as a rectifier in a vehicle that uses regenerative braking.

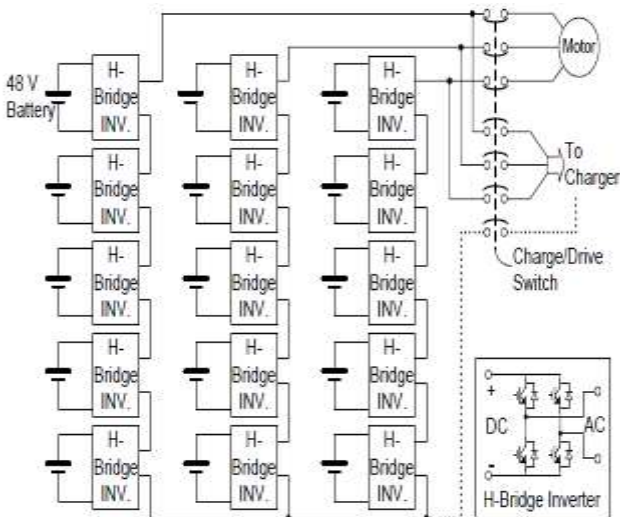


**Figure 10: Three-phase wye-connection structure for electric vehicle motor drive and battery charging.**

The main advantages and disadvantages of multilevel cascaded H-bridge converters are as follows

#### Advantages:

- The number of possible output voltage levels is more than twice the number of dc sources ( $m = 2s + 1$ ).
- The series of H-bridges makes for modularized layout and packaging. This will enable the manufacturing process to be done more quickly and cheaply.

#### Disadvantages:

Separate dc sources are required for each of the H-bridges. This will limit its application to products that already have multiple SDCSs readily available.

#### 3.2 Modeling of Inverter

By considering the inductor currents and capacitor voltage as the state variables of the three-phase grid-connected PV system of Fig. 3, the state-space representation of this system will be

$$\begin{aligned} \dot{i}_a &= -\frac{R}{L}i_a - \frac{1}{L}e_a + \frac{v_{pv}}{3L}(2K_a - K_b - K_c) \\ \dot{i}_b &= -\frac{R}{L}i_b - \frac{1}{L}e_b + \frac{v_{pv}}{3L}(-K_a + 2K_b - K_c) \\ \dot{i}_c &= -\frac{R}{L}i_c - \frac{1}{L}e_c + \frac{v_{pv}}{3L}(-K_a - K_b + 2K_c) \end{aligned}$$

(9) where  $K_a, K_b$  and  $K_c$  are the switching signals related to each phase of three-phase grid connected photovoltaic system.  $i_a, i_b, i_c$  are the output currents from the grid,  $e_a, e_b, e_c$  are the output voltages from the grid [14]. On the other hand, by applying KCL to the DC link capacitor node, the state-space equation for capacitor voltage is obtained as

$$\dot{v}_{pv} = \frac{1}{C}(i_{pv} - i_{dc}) \quad (10)$$

Assuming the switching losses and conduction losses of the inverter to be negligible, the input current of the inverter becomes equal to the output current i.e.

$$i_{dc} = i_a K_a + i_b K_b + i_c K_c \quad (11)$$

which yields,

$$\dot{v}_{pv} = \frac{1}{C}i_{pv} - \frac{1}{C}(i_a K_a + i_b K_b + i_c K_c)$$

(12) Therefore, the state-space model of a lossless three-phase grid-connected PV system can be represented by



$$\begin{aligned} \dot{i}_a &= -\frac{R}{L}i_a - \frac{1}{L}e_a + \frac{v_{pv}}{3L}(2K_a - K_b - K_c) \\ \dot{i}_b &= -\frac{R}{L}i_b - \frac{1}{L}e_b + \frac{v_{pv}}{3L}(-K_a + 2K_b - K_c) \\ \dot{i}_c &= -\frac{R}{L}i_c - \frac{1}{L}e_c + \frac{v_{pv}}{3L}(-K_a - K_b + 2K_c) \\ \dot{v}_{pv} &= \frac{1}{C}i_{pv} - \frac{1}{C}(i_a K_a + i_b K_b + i_c K_c) \end{aligned}$$

(13) The system described by above equations is a non-linear time-varying system due to the nature of switching functions and diode current.

## 4. CONTROL SCHEME

### 4.1 Distributed MPPT Control

In order to eliminate the adverse effect of the mismatches and increase the efficiency of the PV system, the PV modules need to operate at different voltages to improve the utilization per PV module. The separate dc links in the cascaded H-bridge multilevel inverter make independent voltage control possible. To realize individual MPPT control in each PV module, the control scheme proposed in is updated for this application [15]. The distributed MPPT control of the three-phase cascaded H-bridge inverter is shown in Fig. 11. In each H-bridge module, an MPPT controller is added to generate the dc-link voltage reference. Each dc-link voltage is compared to the corresponding voltage reference, and the sum of all errors is controlled through a total voltage controller that determines the current reference  $I_{dref}$ . The reactive current reference  $I_{qref}$  can be set to zero, or if reactive power compensation is required,  $I_{qref}$  can also be given by a reactive current calculator. The synchronous reference frame phase-locked loop (PLL) has been used to find the phase angle of the grid voltage. As the classic control scheme in three-phase systems, the grid currents in abc coordinates are converted to dq coordinates and regulated through fuzzy logic with proportional-integral (PI) controllers to generate the modulation index in the dq coordinates, which is then converted back to three phases. The distributed MPPT control scheme for the single-phase system is nearly the same. The total voltage controller gives the magnitude of the active current reference, and a PLL provides the frequency and phase angle of the active current reference. The current loop then gives the modulation index. To make each PV module operate at its own MPP, take phase a as an example; the voltages  $v_{dc a2}$  to  $v_{dc a n}$  are controlled individually through  $n - 1$  loops. Each voltage

controller gives the modulation index proportion of one H-bridge module in phase a. After multiplied by the modulation index of phase a,  $n - 1$  modulation indices can be obtained. Also, the modulation index for the first H-bridge can be obtained by subtraction.

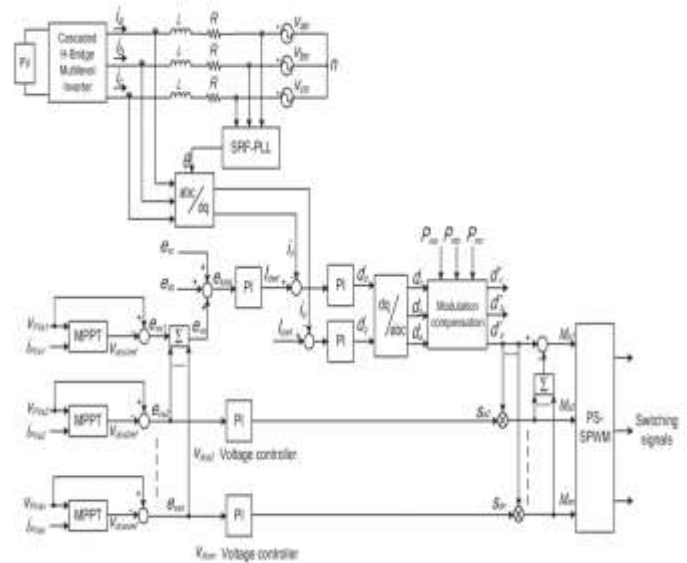


**Figure 11: Control scheme for three-phase modular cascaded H-bridge multilevel PV inverter.**

The control schemes in phases b and c are almost the same. The only difference is that all dc-link voltages are regulated through PI controllers, and  $n$  modulation index proportions are obtained for each phase. A phase-shifted sinusoidal pulse width modulation switching scheme is then applied to control the switching devices of each H-bridge. It can be seen that there is one H-bridge module out of  $N$  modules whose modulation index is obtained by subtraction. For single-phase systems,  $N = n$ , and for three-phase systems,  $N = 3n$ , where  $n$  is the number of H-bridge modules per phase. The reason is that  $N$  voltage loops are necessary to manage different voltage levels on  $N$  H-bridges, and one is the total voltage loop, which gives the current reference. So, only  $N - 1$  modulation indices can be determined by the last  $N - 1$  voltage loops, and one modulation index has to be obtained by subtraction. Many MPPT methods have been developed and implemented. The incremental conductance method has been used in this paper. It lends itself well to digital control, which can easily keep track of previous values of voltage and current and make all decisions.

### 4.2 Modulation Compensation

As mentioned earlier, a PV mismatch may cause more problems to a three-phase modular cascaded H-bridge multilevel PV inverter. With the individual



MPPT control in each H-bridge module, the input solar power of each phase would be different, which introduces unbalanced current to the grid. To solve the issue, a zero sequence voltage can be imposed upon the phase legs in order to affect the current flowing into each phase. If the updated inverter output phase voltage is proportional to the unbalanced power, the current will be balanced. Thus, the modulation compensation block, as shown in Fig. 12, is added to the control system of three-phase modular cascaded multilevel PV inverters. The key is how to update the modulation index of each phase without increasing the

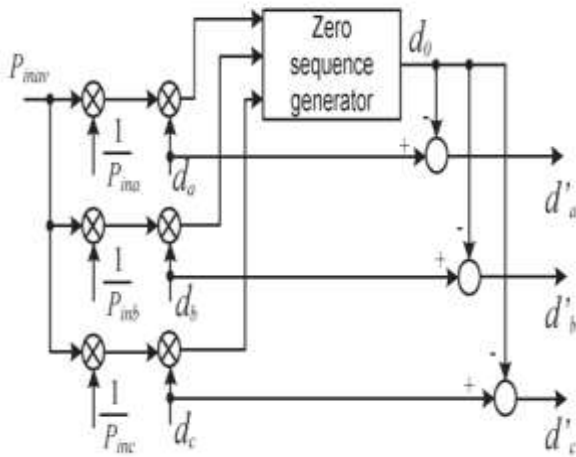


**Figure 12: Modulation compensation scheme.**

complexity of the control system. First, the unbalanced power is weighted by ratio  $r_j$ , which is calculated as

$$r_j = \frac{P_{inav}}{P_{inj}} \quad (14)$$

Where  $P_{inj}$  is the input power of phase  $j$  ( $j = a, b, c$ ), and  $P_{inav}$  is the average input power. Then, the injected zero sequence modulation index can be generated as

$$d_0 = \frac{1}{2} [\min(r_a d_a, r_b d_b, r_c d_c) + \max(r_a d_a, r_b d_b, r_c d_c)] \quad (15)$$

Where  $d_j$  is the modulation index of phase  $j$  ( $j = a, b, c$ ) and is determined by the current loop controller. The modulation index of each phase is updated by

$$d'_j = d_j - d_0 \quad (16)$$

Only simple calculations are needed in the scheme, which will not increase the complexity of the control system. An example is presented to show the modulation compensation scheme more clearly. Assume that the input power of each phase is unequal

$$P_{ina} = 0.8 \quad P_{inb} = 1 \quad P_{inc} = 1 \quad (17)$$

**TABLE 2: System Parameters**

[1] Parameter Specifications	[2] Values
[3] DC link capacitor, C	[4] 3600 $\mu$ F
[5] Connection inductor, L	[6] 2.5 mH
[7] Grid resistor, R	[8] 0.1 ohm
[9] Grid rated phase voltage, V	[10] 60 V <sub>rms</sub>
[11] Switching frequency, f	[12] 1.5 kHz

By injecting a zero sequence modulation index at  $t = 1$  s, the balanced modulation index will be updated, as shown in Fig. 12. It can be seen that, with the compensation, the updated modulation index is unbalanced proportional to the power, which means that the output voltage ( $v_j N$ ) of the three-phase inverter is unbalanced, but this produces the desired balanced grid current.

## 5. SIMULATION RESULTS AND DISCUSSION

### 5.1 Proposed simulation diagrams

Simulation test is carried out to validate the proposed ideas. A modular cascaded multilevel inverter simulation type has been built in the laboratory. The MOSFET IRFSL4127 is selected as inverter switches operating at 1.5 kHz. The control signals to the H-bridge inverters are sent by a fuzzy controller. A three-phase seven-level cascaded H-bridge inverter is simulated as shown in Fig. 13 and Fig. 14. Each H-bridge has its own 185-W PV panel connected as an independent source. The inverter is connected to the grid through a transformer, and the phase voltage of the secondary side is 60 V<sub>rms</sub>. The system parameters are shown in Table 2.

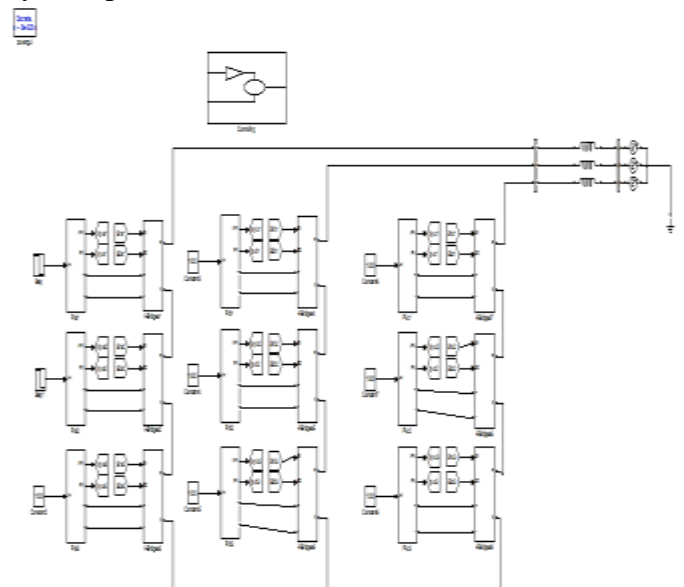


**Figure 13: Proposed simulation diagram**

To verify the proposed control scheme, the three-phase grid connected PV inverter is simulated in two different conditions. First, all PV panels are operated under the same irradiance  $S = 1000 \text{ W/m}^2$  and temperature  $T = 25 \text{ }^\circ\text{C}$ . At  $t = 0.8 \text{ s}$ , the solar irradiance on the first and second panels of phase  $a$  decreases to  $600 \text{ W/m}^2$ , and that for the other panels stays the same. The dc-link voltages of phase  $a$  are shown in Fig. 15. At the beginning, all PV panels are operated at an MPP voltage of  $36.4 \text{ V}$ . As the irradiance changes, the first and second dc link voltages decrease and track the new MPP voltage of  $36 \text{ V}$ , while the third panel is still operated at  $36.4 \text{ V}$ .

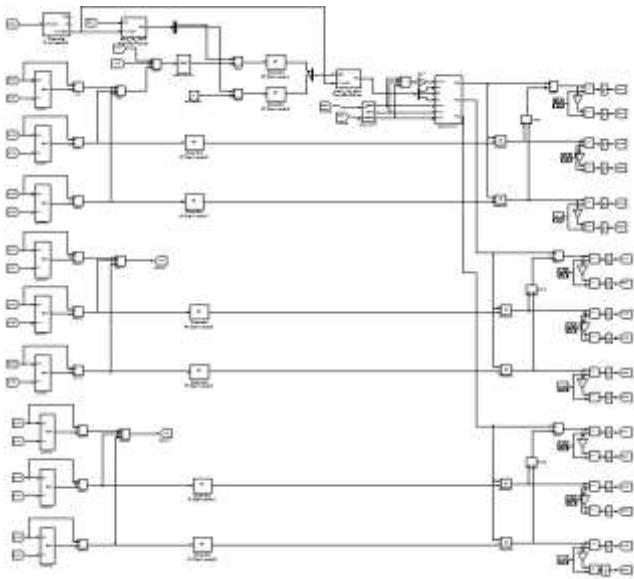


Figure 14: Control structure of proposed system

## 5.2 SIMULATION RESULTS

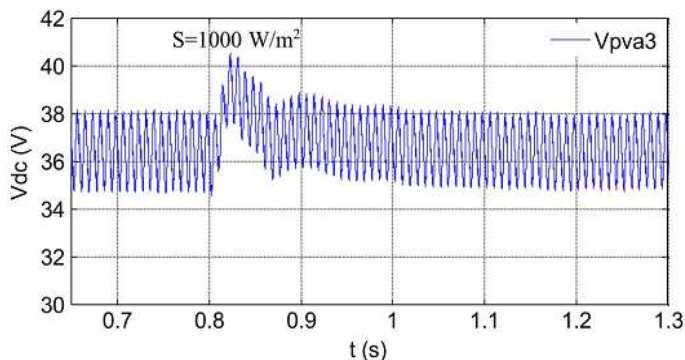


Figure 15: DC-link voltages of phase  $a$  with distributed MPPT ( $T = 25 \text{ }^\circ\text{C}$ ). DC-link voltage of modules 1 and 2.

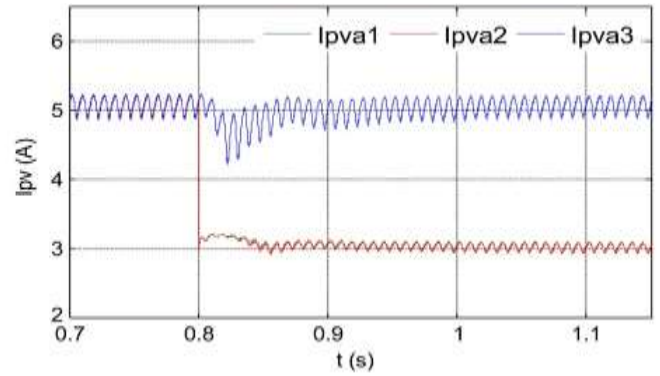


Figure 16: PV currents of phase  $a$  with distributed MPPT ( $T = 25 \text{ }^\circ\text{C}$ )

The PV current waveforms of phase  $a$  are shown in Fig. 16. After  $t = 0.8 \text{ s}$ , the currents of the first and second PV panels are much smaller due to the low irradiance, and the lower ripple of the dc-link voltage can be found in Fig. 17. The dc-link voltages of phase  $b$  are shown in Fig. 17. All phase- $b$  panels track the MPP voltage of  $36.4 \text{ V}$ , which shows that they are not influenced by other phases. With the distributed MPPT control, the dc-link voltage of each H-bridge can be controlled independently. In other words, the connected PV panel of each H-bridge can be operated at its own MPP voltage and will not be influenced by the panels connected to other H-bridges. Thus, more solar energy can be extracted, and the efficiency of the overall PV system will be increased. Fig. 18 shows the power extracted from each phase. At the beginning, all panels are operated under irradiance.

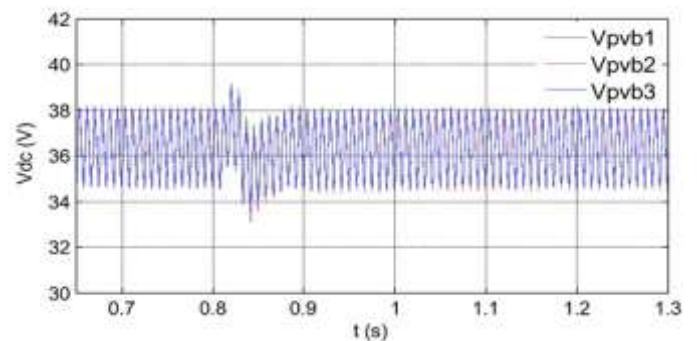


Figure 17: DC-link voltages of phase  $b$  with distributed MPPT ( $T = 25 \text{ }^\circ\text{C}$ ).

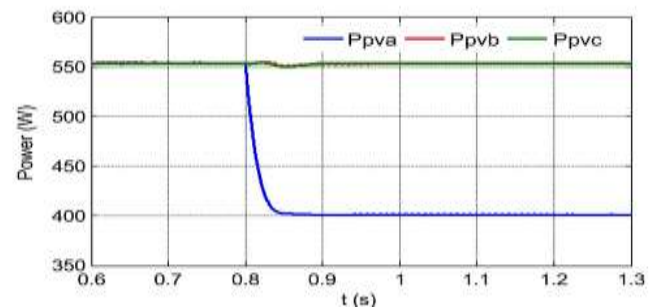
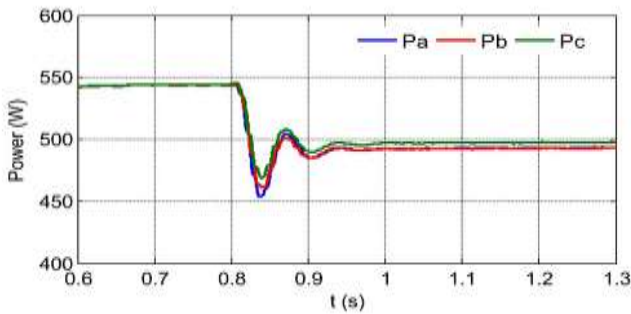
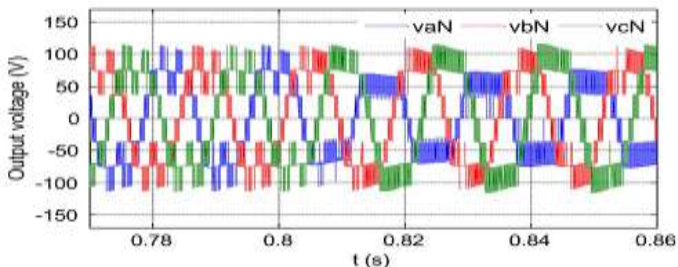


Figure 18: Power extracted from PV panels with distributed MPPT.



**Figure 19: Power injected to the grid with modulation compensation**

$S = 1000 \text{ W/m}^2$ , and every phase is generating a maximum power of 555 W. After  $t = 0.8 \text{ s}$ , the power harvested from phase  $a$  decreases to 400 W, and those from the other two phases stay the same. Obviously, the power supplied to the three-phase grid-connected inverter is unbalanced. However, by applying the modulation compensation scheme, the power injected to the grid is still balanced, as shown in Fig. 19. In addition, by comparing the total power extracted from the PV panels with the total power injected to the grid, it can be seen that there is no extra power loss caused by the modulation compensation scheme. Fig. 20 shows the output voltages ( $v_j N$ ) of the three-phase inverter. Due to the injected zero sequence component, they are unbalanced after  $t = 0.8 \text{ s}$ , which help to balance the grid current shown in Fig. 21.



**Figure 20: Three-phase inverter output voltage waveforms with modulation compensation.**

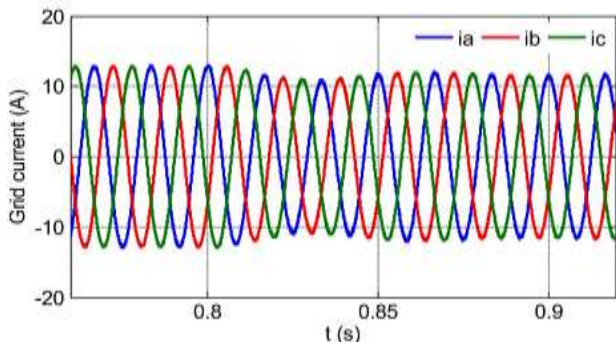


**Figure 21: Three-phase grid current waveforms with modulation compensation.**

The multilevel inverter topology will help to improve the utilization of connected PV modules if the voltages of the separate dc links are controlled

independently. Thus, a distributed MPPT control scheme for both single- and three-phase PV systems has been applied to increase the overall efficiency of PV systems. For the three-phase grid-connected PV system, PV mismatch may introduce unbalanced supplied power, resulting in unbalance injected grid current. A modulation compensation scheme, which will not increase the complexity of the control system or cause extra power loss, is added to balance the grid current.

## 6. Conclusions

In this project, a modular cascaded H-bridge multilevel inverter for grid-connected PV applications has been presented. The multilevel inverter topology will help to improve the utilization of connected PV modules if the voltages of the separate dc links are controlled independently. Thus, a distributed MPPT control scheme for both single- and three-phase PV systems has been applied to increase the overall efficiency of PV systems. For the three-phase grid-connected PV system, PV mismatches may introduce unbalanced supplied power, resulting in unbalance injected grid current. A modulation compensation scheme, which will not increase the complexity of the control system or cause extra power loss, is added to balance the grid current. A modular three-phase seven-level cascaded H-bridge inverter has been built in the laboratory and tested with PV panels under different partial shading conditions. With the proposed control scheme, each PV module can be operated at its own MPPT to maximize the solar energy extraction, and the three-phase grid current is balanced even with the unbalanced supplied solar power.

## 7. References

- [1] Liu, Liming, et al. "Decoupled active and reactive power control for large-scale grid-connected photovoltaic systems using cascaded modular multilevel converters." *IEEE Transactions on Power Electronics* 30.1 (2015): 176-187.
- [2] Rajasekharachari, K., G. Balasundaram, and K. Kumar. Implementation of A Battery Storage System of An Individual Active Power Control Based on A Cascaded Multilevel PWM Converter. *Int J Inno Res Sci Eng Technol.* 2013; 2(7).
- [3] Kumar K, S.V. Sivanagaraju, Rajasekharachari. Single Stage AC-DC Step Up Converter using Boost And Buck-Boost Converters. *Int J Adv Res Electric Electron Instru Eng.* 2013; 2(9): 4245-4252.



- [4] Marquez, Abraham, et al. "Adaptive phase-shifted PWM for multilevel cascaded H-bridge converters with large number of power cells." *Compatibility, Power Electronics and Power Engineering (CPE-POWERENG)*, 2017 11th IEEE International Conference on. IEEE, 2017.
- [5] Zhou, Yan, and Hui Li. "Analysis and suppression of leakage current in cascaded-multilevel-inverter-based PV systems." *IEEE Transactions on Power Electronics* 29.10 (2014): 5265-5277.
- [6] Liu, Yushan, et al. "An effective control method for quasi-Z-source cascade multilevel inverter-based grid-tie single-phase photovoltaic power system." *IEEE Transactions on Industrial Informatics* 10.1 (2014): 399-407.
- [7] Fuentes, Carlos D., et al. "Experimental validation of a single DC bus cascaded H-bridge multilevel inverter for multistring photovoltaic systems." *IEEE Transactions on Industrial Electronics* 64.2 (2017): 930-934.
- [8] Kumar, K., N. Ramesh Babu, and K. R. Prabhu. "Design and Analysis of an Integrated Cuk-SEPIC Converter with MPPT for Standalone Wind/PV Hybrid System." *International Journal of Renewable Energy Research (IJRER)* 7.1 (2017): 96-106.
- [9] Kouro, Samir, et al. "Grid-connected photovoltaic systems: An overview of recent research and emerging PV converter technology." *IEEE Industrial Electronics Magazine* 9.1 (2015): 47-61.
- [10] S. V. Sivanagaraju, K. Kumar, K. Rajasekharachari. Performance Comparison Of Variable Speed Induction Machine Wind Generation System With And Without Fuzzy Logic Controller. *Int J Innov R Devel.* 2013; 2(7).
- [11] Wang, Liang, et al. "Power and voltage balance control of a novel three-phase solid-state transformer using multilevel cascaded H-bridge inverters for microgrid applications." *IEEE Transactions on Power Electronics* 31.4 (2016): 3289-3301.
- [12] Rajasekharachari, K., and K. Shalini, Kumar. K and SR Divya. Advanced Five Level-Five Phase Cascaded Multilevel Inverter with SVPWM Algorithm. *Int J Electric Engi & Technol.* 2013; 4(4): 144-158.
- [13] Yu, Yifan, et al. "Power balance of cascaded H-bridge multilevel converters for large-scale photovoltaic integration." *IEEE Transactions on Power Electronics* 31.1 (2016): 292-303.
- [14] Muthuramalingam, M., and P. S. Manoharan. "Comparative analysis of distributed MPPT controllers for partially shaded stand alone photovoltaic systems." *Energy Conversion and Management* 86 (2014): 286-299.
- [15] Marquez, Abraham, et al. "Variable-Angle Phase-Shifted PWM for Multilevel Three-Cell Cascaded H-Bridge Converters." *IEEE Transactions on Industrial Electronics* 64.5 (2017): 3619-3628.